Magnetic anisotropy of Fe_6 and Fe_{10} molecular rings by cantilever torque magnetometry in high magnetic fields

A. Cornia
Dipartimento di Chimica, Università degli Studi di Modena e Reggio Emilia, via G. Campi 183, 41100 Modena, Italy

A. G. M. Jansen
Grenoble High Magnetic Field Laboratory, Max-Planck-Institut für Festkörperforschung and Centre National de la Recherche Scientifique, Boîte Postale 166, F-38042 Grenoble Cedex 9, France

M. Affronte
Istituto Nazionale per la Fisica della Materia and Dipartimento di Fisica, Università degli Studi di Modena e Reggio Emilia, via G. Campi 213/A, 41100 Modena, Italy

(Received 7 December 1998)

We studied the magnetic anisotropy of two molecular magnets, Fe_6 and Fe_{10}, which comprise six- and ten-membered rings of antiferromagnetically coupled iron (III) ions ($S_i = \frac{5}{2}$), respectively. Spin-flip transitions induced by the applied magnetic field (up to 23 T) were investigated by cantilever torque magnetometry on microgram single crystals at very low temperature (down to 0.45 K). From the sharp, steplike variations of magnetic anisotropy at the transition fields, we determined the singlet-triplet energy gap (Δ_1) and the axial zero-field splitting parameter (D_1) for the triplet state of Fe_6 [$\Delta_1 = 15.28(1)\ cm^{-1}$, $D_1 = 4.32(3)\ cm^{-1}$] and Fe_{10} [$\Delta_1 = 4.479(4)\ cm^{-1}$, $D_1 = 2.24(2)\ cm^{-1}$]. By analyzing the additional steps observed in the Fe_{10} sample, we evaluated the Δ_S and D_S parameters for the total-spin multiplets with S up to 5. On the basis of our findings, we discuss the origin of magnetic anisotropy in iron (III) rings and the application of torque magnetometry to the study of field induced level crossing in molecular magnets. [S0163-1829(99)01041-3]

I. INTRODUCTION

Mesoscopic magnetic systems are attracting increasing interest since they provide the possibility to observe quantum size effects on a macroscopic scale.[1,2] Large magnetic clusters can now be synthesized in bulk quantities by chemical techniques and arranged in a crystal lattice, so that each constituent magnetic object has perfectly defined size and structure.[2] Major achievements in this field have been the observation of quantum tunneling of the magnetization in single-molecule superparamagnets[3] and quantum steps of the magnetization in molecular antiferromagnetic rings.[1,2,4,5] Considerable attention has been focused on the coexistence of classical and quantum effects in large magnetic rings, because the physical properties of a ring are expected to gradually evolve toward those of an infinite chain as the number of interacting spins (N) increases.

In this respect, two high-symmetry iron (III) rings, Fe_6 and Fe_{10}, have been investigated by several different techniques, such as magnetization[4,5] and specific-heat[6] measurements, Mössbauer spectroscopy,[7] and nuclear magnetic resonance.[8,9] In low magnetic fields Fe_6 and Fe_{10} have a nonmagnetic $S=0$ ground state due to dominant antiferromagnetic Heisenberg interactions:

$$\mathbf{H}_H = J\sum_{i=1}^{N} \mathbf{S}_i \cdot \mathbf{S}_{i+1} \tag{1}$$

with $J = 19.9$ and $9.6\ cm^{-1}$ in the two compounds, respectively.[4,5] As observed in infinite chains, these systems are characterized by a critical slowing down of electron-spin fluctuations at temperatures close to J/k_B.[8] However, quantum size effects are manifest in the regular staircase structure of magnetization curves measured at $T<1$ K as a function of magnetic field. The origin of the steps and their different field spacing in the two compounds (16.4 and 4.7 T, respectively)[4,5] are reasonably well understood in terms of spin-flip transitions induced by the applied magnetic field (see Appendix).

Although non-Heisenberg terms are generally assumed to be distinctly smaller than the dominant exchange Hamiltonian (1), recent theoretical investigations on the spin dynamics of Fe_6 and Fe_{10} clusters have evidenced a subtle interplay between finite size effects and non-Heisenberg interactions.[1,7,9]

For this reason, we undertook a detailed investigation of magnetic anisotropy on single-crystal samples of Fe_6 and Fe_{10} by using high-field torque magnetometry. Torque magnetometry with its many variations (critical-couple or flip-angle method, null-deflection,[10] and cantilever methods[11]) was one of the first techniques developed for measuring magnetic anisotropy. Suitably coupled with an average susceptibility measurement, it has been widely used for the determination of principal susceptibilities in simple paramagnets,[10,12] but high-field applications have been developed only recently.[11] The torque $\mathbf{T}$ experienced by a magnetically anisotropic substance in a uniform magnetic field $\mathbf{B}$ is given by[10]

$$\mathbf{T} = \mathbf{M} \times \mathbf{B}, \tag{2}$$

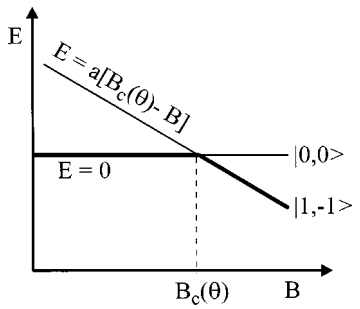

FIG. 1. Simplified spin-level scheme for singlet-triplet crossing.

where **M** is the magnetization of the sample. **T** vanishes when the magnetic field is applied along one of the principal directions *x*,*y*,*z* of the susceptibility tensor (χ), since in this case **M** and **B** are collinear. Typically, the rotation axis of the torquemeter is set parallel to *y* while **B** is applied in the *xz* plane at an angle θ from *z*, so that the *y* component of the torque vector is given by

$$T_y = B^2(\chi_{zz} - \chi_{xx})\sin\theta\cos\theta. \tag{3}$$

Equation (3) shows that for a given orientation of the field the torque signal is proportional to the in-plane anisotropy and to the square of the magnetic-field modulus, so that sensitivity increases dramatically in high magnetic fields. However, a different behavior is expected for Fe_6 and Fe_{10} in the low-temperature regime due to field induced modulation of the ground state. In order to illustrate this point we recall that, in the limit of dominant Heisenberg contributions (1), the effect of magnetic anisotropy and Zeeman interactions on each *S* multiplet is described by the spin Hamiltonian[13]

$$\mathbf{H}_S = \mathbf{S}\cdot\mathbf{D}_S\cdot\mathbf{S} + g\mu_B\mathbf{B}\cdot\mathbf{S}. \tag{4}$$

As a consequence of Eq. (4), in an anisotropic system the magnetic-field values (B_c) required for spin-flip transitions are θ dependent (see Appendix). The problem of singlet-triplet level crossing in a ring with axial symmetry (*z* unique) can be solved analytically by direct diagonalization of the 3×3 spin-Hamiltonian matrix for the $S=1$ multiplet:[13,14]

$$B_c(\theta) = \frac{\Delta_1 + \frac{1}{3}D_1}{g\mu_B}\left(\frac{\Delta_1 - \frac{2}{3}D_1}{\Delta_1 + \frac{1}{3}D_1(1 - 3\cos^2\theta)}\right)^{1/2}. \tag{5}$$

In Eq. (5), D_1 and Δ_1 are the zero-field splitting parameter of the triplet state and the singlet-triplet energy gap, respectively. One notices that the trend of B_c values is qualitatively related to the sign of D_1, because $B_c(90) < B_c(0)$ when $D_1 > 0$ while the opposite holds when $D_1 < 0$. Since the $|0,0\rangle$ state is magnetically isotropic, the torque signal observed at magnetic field values close to $B_c(\theta)$ (Fig. 1) must reflect contributions from the $|1,-1\rangle$ state only. We can safely assume a linear field dependence of the energy of $|1,-1\rangle$ around the crossing point B_c, so that the thermal expectation value of T_y is simply given by

$$\langle T_y\rangle = \langle 1,-1|\mathbf{T}_y|1,-1\rangle\left[1 + \exp\left(-a\frac{B - B_c(\theta)}{k_BT}\right)\right]^{-1}, \tag{6}$$

where $-a$ is the slope of $|1,-1\rangle$ at $B = B_c(\theta)$, while $\mathbf{T}_y$ is the *y* component of the torque operator $\mathbf{T}_y = -(\partial\mathbf{H}_S/\partial\theta)_B$. According to Eq. (6), $\langle T_y\rangle$ should exhibit a steplike field dependence with inflection point at $B_c(\theta)$. Furthermore, the width of the step should be simply proportional to the absolute temperature:

$$\mathrm{FWHM} = \left(\frac{k_BT}{a}\right)\ln\left(\frac{3+2\sqrt{2}}{3-2\sqrt{2}}\right). \tag{7}$$

In this work, we used a cantilever torque method in high magnetic fields (0–23 T) to study the angular dependence of the critical fields required for spin-flip transitions at low temperature (0.45 K). As anticipated in a previous report,[4] our approach provides considerable information on the zero-field splitting parameters of exchange multiplets and on the origin of magnetic anisotropy. More generally, we show how this technique can be successfully used to study level crossing in magnetic materials and to determine the zero-field splitting of excited multiplets, which is usually obtained through electron paramagnetic resonance (EPR) spectroscopy.[13]

The paper is organized as follows. In Sec. II we discuss the experimental details while in Sec. III we present the experimental results. In Sec. IV we analyze the field dependence of the torque signal in terms of spin level crossing and relate the observed critical fields to the spin-Hamiltonian parameters. Finally, in Sec. V we draw conclusions.

II. EXPERIMENTAL DETAILS

A high-sensitivity Cu/Be cantilever mounted on a ^{3}He cryostat was used for the torque measurements. The experimental apparatus, shown in Fig. 2(a), was sensitive to the *y* component of the torque vector (T_y) acting on the sample in a magnetic field **B**, which was applied in the *xz* plane at an angle θ from *z*. Rotations of the sample were performed around the *y* axis. The deflection of the cantilever with respect to the zero-field position was detected by measuring the capacitance of the torquemeter (*C*), assuming $C \propto 1/d$ [see Fig. 2(a)]. Capacitance variations (ΔC) during the experiments were less than 0.5% of the zero-field capacitance (about 1.0 pF), so that a simple proportionality between ΔC and T_y was assumed. Temperature was monitored by using a calibrated RuO_2-based resistor and the thermal stability of the system was within 50 mK in the range 4.3–0.45 K. Magnetic fields up to 23 T were applied by using one of the polyhelix electromagnets available at the High Magnetic Field Laboratory in Grenoble, with field-sweep rates in the range 400–600 G/s which led to insignificant hysteresis effects.

10-μg single crystals of Fe_6 and Fe_{10} were synthesized by literature procedures.[4,5] Fe_6 crystallizes in space group $R\bar{3}$ and forms red needles with a well developed trigonal symmetry. The rings are iso-oriented in the crystal, with their sixfold axes lying parallel to the needle *c* axis [Fig. 2(b)]. The selected single crystal (approximate dimensions: $0.35\times0.15\times0.15$ mm) was mounted on the cantilever under an optical stereomicroscope, with the *c* axis parallel to *z* and the (100) face lying on the metal surface. Consequently, the field was applied in the a^*c plane [Fig. 2(b)], while the θ angle between the magnetic field and the *c* axis was experimentally

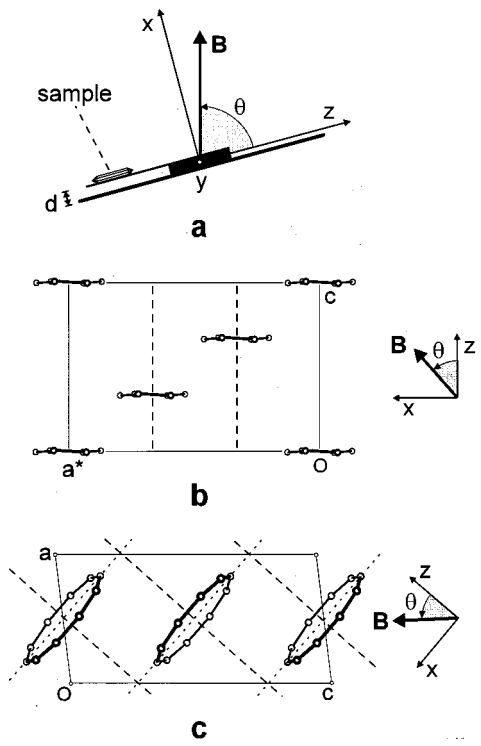

FIG. 2. (a) Side view of the cantilever torquemeter with the coordinate system used in the experiments. (b) Projection of the crystal structure of Fe_6 onto the a^*c plane of the trigonal unit cell (hexagonal setting). (c) Projection of the crystal structure of Fe_{10} onto the *ac* plane of the monoclinic unit cell. In both (b) and (c), only iron (III) atoms are shown for clarity. The traces of sixfold and idealized tenfold molecular axes are depicted by dashed lines.

varied in the range 0–90°. The crystal was covered with silicon grease in order to prevent solvent loss during the room-temperature mounting. A similar procedure was used for the Fe_{10} compound, which crystallizes in monoclinic space group $P2_1/c$ and forms small yellow prisms. The two planar Fe_{10} molecules present in the unit cell are related by the 2_1 screw axis directed along *b* and form a dihedral angle $\alpha = 21.1°$ between themselves [Fig. 2(c)]. Due to the irregular shape of the crystals, the orientation of the unit-cell vectors in the selected individual (approximate dimensions: $0.25 \times 0.20 \times 0.10$ mm) was determined by combined use of a polarizing microscope and an ENRAF Nonius CAD-4 κ-geometry diffractometer. The unique *b* axis was optically aligned parallel to *y* and the magnetic field was applied in the *ac* plane [Fig. 2(c)]. The angle θ between the magnetic field and the *z* direction, defined by the traces of the idealized tenfold ring axes, was varied in the range 10 to $-95°$. The estimated accuracy of the adopted alignment procedure is $\pm 5°$.

III. EXPERIMENTAL RESULTS

(a) Fe_6 sample. The *y* component of the torque vector acting on the crystal in a magnetic field **B** (T_y) was detected by measuring the capacitance variation of the torquemeter $\Delta C \propto T_y$ as a function of magnetic field, temperature, and orientation of the sample [Fig. 2(b)]. Curves recorded at $T = 4.3$, 1.4, 0.70, and 0.45 K for $\theta = 45°$ are shown in Fig. 3.

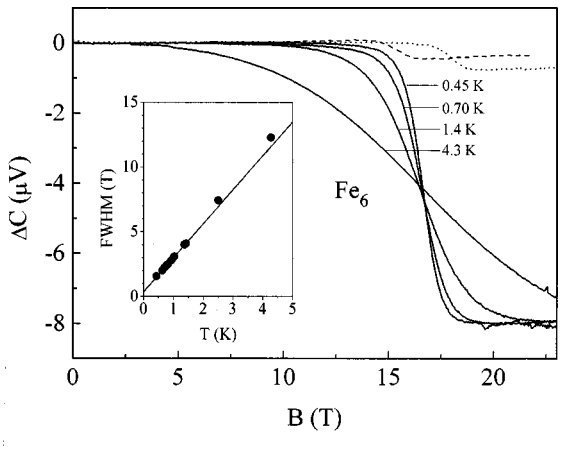

FIG. 3. Torque curves recorded on the Fe_6 single crystal at $T = 0.45–4.3$ K and $\theta = 45°$ (solid lines), at $T = 0.45$ K and $\theta = 90°$ (dashed line), and at $T = 0.45$ K and $\theta = 5°$ (dotted line). The inset shows the temperature dependence of the full width at half maximum (FWHM) of the step.

As anticipated in Sec. I, the torque signal exhibits a steplike field dependence which becomes more pronounced at the lowest temperatures. Further, the orientation of the sample does not simply modulate the overall intensity of the signal, as predicted by Eq. (3), but also affects the position of the steps (Figs. 3 and 4). The decrease of the capacitance implies $T_y < 0$ and directly provides the sign of magnetic anisotropy, pointing to the presence of a *hard* magnetic axis along *c*. Although the inflection point of the step (B_c), evaluated from the first derivative curves, is the same at all temperatures, the full width at half maximum (FWHM) increases from 1.56 T at 0.45 K to about 12.3 T at 4.3 K (inset to Fig. 3). For $T < 1$ K, however, the thermal broadening of the step is small enough to reveal a smooth shift of B_c as a function of θ (Fig. 3). In Fig. 4 we plot the θ dependence of B_c measured at 0.70 K (the θ values have been translated to the familiar 0–90° range). We notice that when **B** is virtually parallel to the crystallographic *c* axis ($\theta = 0°$) the step occurs at higher fields (17.9 T) as compared to the perpendicular

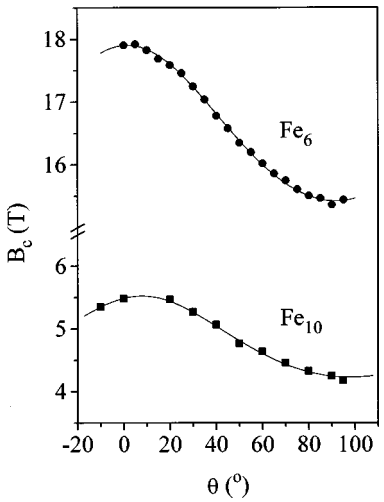

FIG. 4. Angular dependence of the inflection point (B_c) for the first torque step measured at 0.70 and 0.45 K on the Fe_6 and Fe_{10} single crystals, respectively.

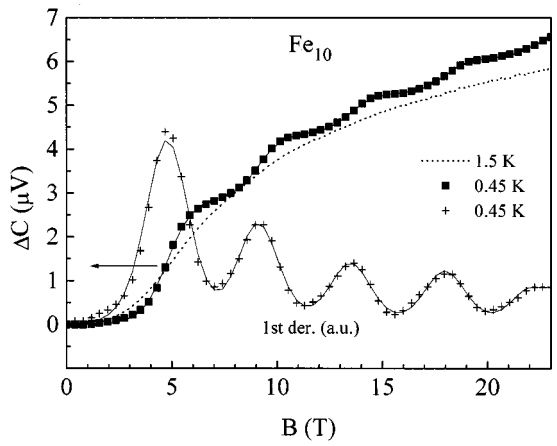

FIG. 5. Torque curves measured at 1.5 and 0.45 K on the Fe_{10} single crystal at $\theta = -49.8°$. The solid line gives the best-fit curve to 0.45-K data. The first derivatives of experimental and calculated curves are also shown.

orientation (15.4 T). Furthermore, the torque signal vanishes when θ is close to $n\pi/2$ (n integer), which represent principal magnetic directions in the crystal.

(b) Fe_{10} sample. The torque signal on the Fe_{10} sample was studied at different temperatures by applying the magnetic field at $\theta = -49.8°$ [Fig. 2(c)]. At 0.45 K, four steps centered at 4.8, 9.2, 13.6, and 18.0 T can be clearly resolved (Fig. 5). The steps have similar width among each other and the FWHM of the first step (1.60 T) is comparable with that found in the six-membered ring at the same temperature (1.56 T). The steps rapidly merge into a broad feature as the temperature is increased above 1 K. We observed vanishing torque signals for θ close to 0 and 90°, which must therefore correspond to principal magnetic directions in the *ac* plane. The increase of the capacitance implies $T_y > 0$ and points to the presence of a *hard* magnetic axis along z [Fig. 2(c)]. The pattern of B_c values for the first step at 0.45 K, plotted in Fig. 4 as a function of θ, looks quite similar to that found in the Fe_6 sample, with critical fields in the range 4.2–5.6 T (as in the Fe_6 case, the θ values have been translated to the 0–90° range).

IV. DISCUSSION

The spin-Hamiltonian parameters were determined from the observed angular dependence of B_c making use of Eq. (5). D_1, Δ_1, and a θ offset (θ_0) were used as adjustable parameters, while the g factor was fixed at 2.00. Notice that the experimental θ values for Fe_{10} were replaced by the true angles between **B** and the idealized tenfold cluster axes. The best-fit parameters are collected in Table I. The D_1 and Δ_1 parameters in Fe_6 are in good agreement with the results of a previous high-field magnetization studies on powder samples.[4] The D_1 value in Fe_{10} is surprisingly large if compared with the singlet-triplet gap Δ_1, so that the validity of Eq. (4) for this compound can be questioned. The best-fit θ_0 value in Fe_{10} also shows that the axial approximation, although not crystallographically dictated, is realistic as suggested by a careful inspection of molecular geometry.[5]

The four additional steps observed on the Fe_{10} sample in high fields were associated with level crossings involving

TABLE I. Spin-Hamiltonian parameters for the triplet state of Fe_6 and Fe_{10}.

	Fe_6		Fe_{10}	
Δ_1 (cm^{-1})	15.28(1)[a]	15.2,[b] 13.7[c]	4.479(4)[a]	4.24,[b] 3.84[c]
D_1 (cm^{-1})	4.32(3)[a]	4.0[c]	2.24(2)[a]	
θ_0 (°)	−1.6(4)[a]		7.7(1)[a]	
g[d]	2.00		2.00	

[a]This work.
[b]From high-field magnetization studies on powder samples (Refs. 4 and 5).
[c]From low-field χ vs T data (Refs. 4 and 5).
[d]Held fixed.

excited exchange multiplets with $S > 1$. Our approach consisted in directly fitting the T_y vs B curve recorded at 0.45 K and $\theta = -49.8°$, which showed best-resolved steps and maximum signal intensity (Fig. 5). For each set of spin-Hamiltonian parameters, the T_y vs B curve was calculated numerically from the matrix elements of $\mathbf{T}_y$ and Boltzmann statistics, as described in the Appendix. In Table II we collect the best-fit spin-Hamiltonian parameters that we obtained by setting $D_1 = 2.24$ and $g = 2.00$. In order to reproduce the step width, we also treated temperature as an adjustable parameter [$T = 0.76(1)$ K]. It is essential to notice that the significance of our multivariable fit lies in the different influence of D_S and Δ_S on the torque curves. More precisely, the height of each step is mainly determined by the D_S/D_{S+1} ratio, whereas the inflection point is related to both D_S and Δ_S values.

The quantity $(\Delta_S - \Delta_{S-1})/S$, reported in Table II, shows that the Landé interval rule is obeyed within experimental error for $S > 1$. This is to be compared for instance with the marked deviations observed for Mn^{2+} pairs in CuO, which required the introduction of large biquadratic exchange effects.[15]

The positive sign of D_S points to a *hard axis* magnetic anisotropy in both systems. The trend of D_S parameters in Table II compares well with that predicted for either dominant single-ion or dipolar contributions to magnetic anisotropy (fifth and sixth column, respectively).[13] For dominant crystal-field terms, the measured D_1 values in Fe_6 and Fe_{10} can be used to estimate single-ion anisotropies by standard projection techniques.[4,13] Defining single-ion anisotropies through spin-Hamiltonian

TABLE II. Exchange energies and zero-field splitting parameters (cm^{-1}) for the Fe_{10} sample.

				D_S	
S	Δ_S	$(\Delta_S - \Delta_{S-1})/S$	expt	single ion[a]	dipolar[a]
1	4.43(1)	4.43(1)	2.24(2)[b]		
2	12.78(3)	4.17(2)	0.599(3)	0.524	0.540
3	25.28(5)	4.17(2)	0.291(1)	0.238	0.256
4	41.98(8)	4.17(2)	0.180(1)	0.134	0.153
5	62.6(2)	4.12(4)	0.123(1)	0.084	0.103

[a]Calculated assuming $D_1 = 2.24\ cm^{-1}$ and $g = 2.00$.
[b]Determined from B_c vs θ data and held fixed.

$$\mathbf{H}_{Fe}=\overline{k}_{Fe}(\mathbf{S}_z^2-\tfrac{1}{3}\mathbf{S}^2) \tag{8}$$

we obtain $\overline{k}_{Fe}=-0.3\,cm^{-1}$ in Fe_6 and -0.1 cm^{-1} in Fe_{10}. This result is in contrast with a recent report by Chiolero and Loss on the semiclassical spin dynamics of antiferromagnetic rings.[1] The authors showed that for $\theta=90°$ and $\overline{k}_{Fe}>0$ (i.e., $D_S<0$) the width of the steps should reflect the tunneling dynamics of the Néel vector,[1] and they encouraged single-crystal studies on Fe_{10} in order to support these theoretical predictions. We now find that $\overline{k}_{Fe}<0$ and $D_S>0$ in Fe_{10}, which does not match the tunneling scenario discussed in Ref. 1. Interestingly, three additional antiferromagnetic rings recently investigated by torque magnetometry and high-frequency EPR, namely $[LiFe_6(OCH_3)_{12}(dbm)_6]PF_6$,[16] $[Fe_8F_8(t\text{-}BuCO_2)_{16}]$,[17] and $[Fe_6(tea)_6]$,[18] showed a *hard axis* magnetic anisotropy as well, despite the different chemical environment of the metal ions. For this reason, we checked to which extent the assumption of dominant crystal-field contributions may be realistic. On the basis of the observed Fe-Fe distances[19] and in the point-dipole approximation,[13] the contribution of intramolecular dipolar interactions to D_1 is $D_1^{dip}=1.15\,cm^{-1}$ in Fe_6 and 2.24 cm^{-1} in Fe_{10}. Hence, dipolar terms sum up to 26% of the D_1 value observed in Fe_6, and entirely account for the measured triplet splitting in Fe_{10}. We are led to the conclusion that dipolar interactions provide a substantial contribution to magnetic anisotropy in these molecular clusters.

Finally, we comment on the FWHM vs T data at $T<1.5\,K$ (inset to Fig. 3). The best-fit value $a=0.932(11)\,cm^{-1}/T$ resulting from Eq. (7) is in excellent agreement with that expected for singlet-triplet crossing ($a\sim-g\mu_B S=0.934\,cm^{-1}/T$ with $g=2.00$), pointing to dominant thermal broadening of the steps. However, the best-fit line in the inset to Fig. 3 has nonzero intercept. In fact the step width in both Fe_6 and Fe_{10} at 0.45 K ($\sim$1.6 T) is larger than expected for simple thermal broadening (1.18 T). The excess width ($\sim$0.4 T) may be an artifact due to misalignment between microscopic crystal domains (mosaicity). The sensitivity of B_c to the θ angle is infact maximum for θ close to $\pm45°$ (see Fig. 4). Our interpretation is consistent with the narrower steps observed in Fe_6 for θ approaching 0 and 90° [FWHM$=1.30(4)$ T at 0.45 K].

V. CONCLUDING REMARKS

We investigated magnetic anisotropy in two molecular clusters with a ringlike structure, Fe_6 and Fe_{10}. Spin-flip transitions were induced by applying magnetic fields up to 23 T and were followed by cantilever torque magnetometry on microgram single crystals at low temperature. The smooth angular variation of transition fields provided a detailed picture of low-lying spin states in these antiferromagnetic clusters (Tables I and II), showing that in both Fe_6 and Fe_{10} the ring axis represents a *hard* magnetic axis. On this basis, we suggest that dipolar interactions may provide a substantial contribution to the observed anisotropy. The zero-field splitting parameters observed in Fe_6 and Fe_{10} confirm that polynuclear iron (III) compounds may exhibit fairly large magnetic anisotropies and represent good candidates for the observation of superparamagneticlike behavior.[2,3]

We finally stress that the main advantage of our approach, as compared with low-field susceptibility measurements at variable temperature,[4] lies in the absence of thermal averaging effects on the different multiplets, which mix individual contributions to magnetic anisotropy. In this respect, the information extracted from our single-crystal studies is *quasispectroscopic* in quality. High-field torque magnetometry thus provides a general tool for the study of magnetic anisotropy in antiferromagnetic spin-structures, with possible applications in the field of superconducting cuprates and spin-Peierl's compounds.

ACKNOWLEDGMENTS

The authors thank Professor D. Gatteschi and Dr. R. Sessoli (Università degli Studi di Firenze) for invaluable discussion. We gratefully acknowledge the contributions of Professor A. C. Fabretti, Professor R. Grandi (Università degli Studi di Modena e Reggio Emilia), and Dr. A. Caneschi (Università degli Studi di Firenze) to the preparation of single-crystal samples. This work was in part financially supported through the TMR Program of the European Community under Contract No. ERBFMGECT950077.

APPENDIX: SPIN HAMILTONIAN FOR MAGNETIC RINGS

The low-temperature physics of a N-membered ring is ruled by Hamiltonian

$$\mathbf{H}=J\sum_{i=1}^{N}\mathbf{S}_i\cdot\mathbf{S}_{i+1}+\sum_{i=1}^{N}U_i(\mathbf{S}_i)+\sum_{i\neq j}^{N}U_{i,j}(\mathbf{S}_i,\mathbf{S}_j)$$
$$+g\mu_B\mathbf{B}\cdot\sum_{i=1}^{N}\mathbf{S}_i \tag{A1}$$

which includes nearest-neighbor (NN) Heisenberg interactions (first term), magnetocrystalline anisotropies (second term), dipolar or anisotropic-exchange contributions (third term) and Zeeman interactions (fourth term). In Eq. (A1), $\mathbf{S}_{N+1}=\mathbf{S}_1$ and higher-order terms in the spin variables have been neglected.[1] The y component of the torque operator $\mathbf{T}_y$ can be easily obtained by differentiating the Zeeman term in Eq. (A1) with respect to the angular variable (θ) describing the rotation around the y axis:

$$\mathbf{T}_y=-\left(\frac{\partial\mathbf{H}}{\partial\theta}\right)_B=-g\mu_B B\sum_{i=1}^{N}(\mathbf{S}_i^x\cos\theta-\mathbf{S}_i^z\sin\theta)$$
$$=-g\mu_B B(\mathbf{S}^x\cos\theta-\mathbf{S}^z\sin\theta), \tag{A2}$$

where $\mathbf{S}=\Sigma_{i=1}^{N}\mathbf{S}_i$ is the total-spin operator. The matrix elements of $\mathbf{T}_y$ must then be computed on the basis of eigenvectors of Hamiltonian (A1) and the thermal expectation value of $\mathbf{T}_y$ evaluated by using Boltzmann statistics.

Different approaches have been proposed to solve Hamiltonian (A1) for an antiferromagnetic ring. Since the dimensions of the Hamiltonian matrix $[(2S_i+1)^N\times(2S_i+1)^N]$ increase very rapidly with N, for large S_i full diagonalization becomes a formidable task even when the number of interacting spins is small. In the case of Fe_6 and Fe_{10}, for instance, the dimensions of the full Hamiltonian matrix are

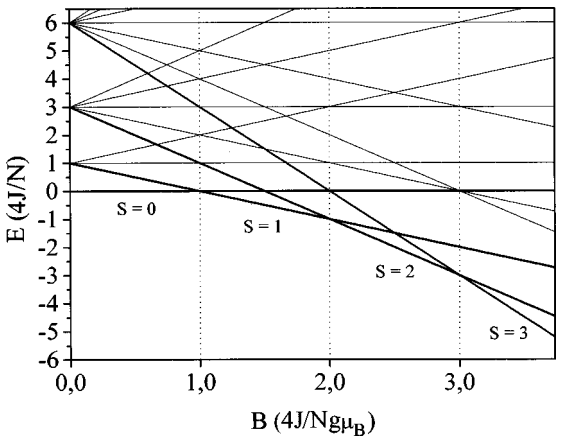

FIG. 6. Spin-level scheme for the low-lying multiplets in an antiferromagnetic ring, showing multiple level crossing induced by the applied magnetic field. The total-spin ground state S in each field interval is also reported.

$46\,656\times 46\,656$ and $60\,466\,176\times 60\,466\,176$, respectively. An alternative semiclassical approach has been recently proposed to solve Eq. (A1) in the general case.[1] However, considerable simplification of the problem is possible when Heisenberg interactions (1) represent the leading term in Eq. (A1). In this case, the Heisenberg matrix can be block factorized by exploiting the symmetry properties of the total spin $\mathbf{S}$,[20] and rings of $S_i=\frac{5}{2}$ spins with N up to 8 can be easily handled. For instance, $N=6$ leads to 16 matrices with size ranging from 1×1 to 609×609 and S values ranging from 15 to 0. It is a general result that when N is even and S_i is large, the low-lying exchange multiplets have only the magnetic degeneracy $(2S+1)$, and their energies are approximated by the expression

$$E_S=\frac{J'}{2}S(S+1), \tag{A3}$$

where $J'\sim 4J/N$ corresponds to the singlet-triplet energy gap. We have extensively discussed elsewhere the validity of Eq. (A3),[4,21] which is a statement of the Landé interval rule[13] and provides a good starting point for the investigation of large rings. Experimentally, Eq. (A3) accounts for the evenly-spaced steps observed in the M vs B curves of Fe_6 and Fe_{10} at low temperature. As illustrated in Fig. 6, field induced level crossing occurs at critical fields

$$B_c=J\frac{4(S+1)}{Ng\mu_B}, \tag{A4}$$

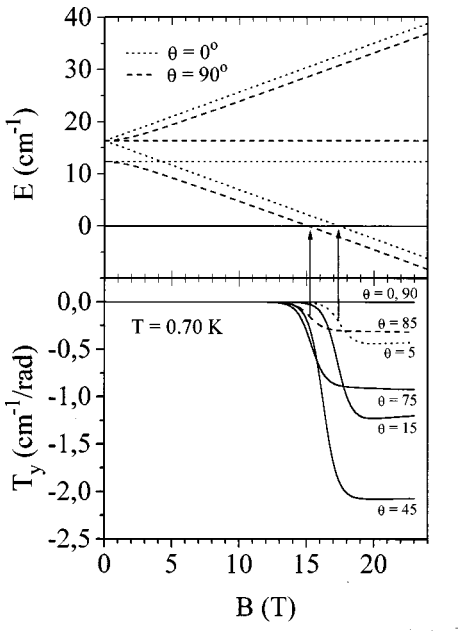

FIG. 7. Upper panel: level diagram showing the angular dependence of level-crossing fields between singlet (solid line at $E=0$) and triplet states (broken lines) for $D_1=4\ \mathrm{cm}^{-1}$, $\Delta_1=15\ \mathrm{cm}^{-1}$, and $g=2.00$. Lower panel: calculated torque curves for the same set of spin-Hamiltonian parameters and representative values of θ at $T=0.70$ K.

whereupon the spin ground state changes from S to $S+1$ at regular field intervals. In this approach, non-Heisenberg contributions can be easily handled through perturbative Hamiltonians (4) acting on the different multiplets. Similarly, calculation of the matrix representative of $\mathbf{T}_y$ [Eq. (A2)] simplifies considerably because it can be carried out separately for each multiplet. In Fig. 7 we focus on singlet-triplet crossing and plot calculated T_y vs B curves for $T=0.7$ K, $D_1=4.0\ \mathrm{cm}^{-1}$, $\Delta_1=15.0\ \mathrm{cm}^{-1}$ and $g=2.00$ (lower panel). For the sake of clarity, in the same figure (upper panel) we also plot the field dependence of the ground singlet $(S=0)$ and of the excited triplet $(S=1)$ levels when the magnetic field is applied parallel $(\theta=0°)$ and perpendicular $(\theta=90°)$ to the anisotropy axis. The angular modulation of the signal nicely agrees with the experimental one. In particular, the signal vanishes when the field is parallel $(\theta=0°)$ and perpendicular $(\theta=90°)$ to the anisotropy axis, as expected due to the axial symmetry. Moreover, the inflection point shifts by changing the orientation of the magnetic field, following the variation in the critical field B_c required for level crossing.

[1] A. Chiolero and D. Loss, Phys. Rev. Lett. **80**, 169 (1998).
[2] D. Gatteschi, A. Caneschi, A. Cornia, and R. Sessoli, Chem. Soc. Rev. **25**, 101 (1996).
[3] W. Wernsdorfer and R. Sessoli, Science **284**, 133 (1999), and references therein.
[4] A. Caneschi, A. Cornia, A. C. Fabretti, S. Foner, D. Gatteschi, R. Grandi, and L. Schenetti, Chem.-Eur. J. **2**, 1379 (1996).
[5] K. L. Taft, C. D. Delfs, G. C. Papaefthymiou, S. Foner, D. Gatteschi, and S. J. Lippard, J. Am. Chem. Soc. **116**, 823 (1994).
[6] M. Affronte, A. Cornia, A. Caneschi, and J. C. Lasjaunias, Phys. Rev. B **60**, 1161 (1999).
[7] Z. Zeng, Y. Duan, and D. Guenzburger, Phys. Rev. B **55**, 12 522 (1997); A. Caneschi, M. Capaccioli, L. Cianchi, A. Cornia, F. DelGiallo, F. Pieralli, and G. Spina, Hyperfine Interact. **116**, 215 (1998).
[8] A. Lascialfari, Z. H. Jang, F. Borsa, D. Gatteschi, and A. Cornia, J. Appl. Phys. **83**, 6946 (1998); A. Lascialfari, D. Gatteschi, F. Borsa, and A. Cornia, Phys. Rev. B **55**, 14 341 (1997); A. Las-

cialfari, D. Gatteschi, A. Cornia, U. Balucani, M. G. Pini, and A. Rettori, *ibid.* **57**, 1115 (1998).

[9] M.-H. Julien, Z. H. Jang, A. Lascialfari, F. Borsa, M. Horvatic, A. Caneschi, and D. Gatteschi, Phys. Rev. Lett. **83**, 227 (1999).

[10] W. De W. Horrocks, Jr., and D. De. W. Hall, Coord. Chem. Rev. **6**, 147 (1971); S. Mitra, Prog. Inorg. Chem. **22**, 309 (1977).

[11] M. Chaparala, O. H. Chung, and M. J. Naughton, in *Superconductivity and its Applications*, Proceedings of the Sixth Annual Conference, Buffalo, 1992, edited by H. S. Kwok, D. T. Shaw, and M. J. Naughton, AIP Conf. Proc. No. 273 (AIP, New York, 1992), p. 407; M. J. Naughton, J. P. Ulmet, and M. Chaparala, Bull. Am. Phys. Soc. **41**, 302 (1996); S. Uji, M. Chaparala, S. Hill, P. S. Sandhu, J. Qualls, L. Seger, and J. S. Brooks, Synth. Met. **85**, 1573 (1997); J. A. A. J. Perenboom, J. S. Brooks, S. O. Hill, T. Hathaway, and N. S. Dalal, Physica B **246-247**, 294 (1998); J. A. A. J. Perenboom, J. S. Brooks, S. O. Hill, T. Hathaway, and N. S. Dalal, Phys. Rev. B **58**, 330 (1998).

[12] R. L. Carlin, *Magnetochemistry* (Springer-Verlag, Berlin, 1986).

[13] A. Bencini and D. Gatteschi, *EPR of Exchange Coupled Systems* (Springer-Verlag, Berlin, 1990).

[14] J. S. Griffith, *The Theory of Transition Metal Ions* (Cambridge University Press, Cambridge, England, 1961).

[15] E. A. Harris, J. Phys. C **5**, 332 (1972).

[16] G. L. Abbati, A. Cornia, A. C. Fabretti, W. Malavasi, L. Schenetti, A. Caneschi, and D. Gatteschi, Inorg. Chem. **36**, 6443 (1997); A. Cornia, M. Affronte, A. G. M. Jansen, G. L. Abbati, and D. Gatteschi, Angew. Chem. Int. Ed. Engl. **38**, 2261 (1999).

[17] A. Cornia, E. Rentschler, A. G. M. Jansen, and M. Affronte (unpublished).

[18] B. Pilawa, R. Desquiotz, M. T. Kelemen, M. Weickenmeier, and A. Geisselmann, J. Magn. Magn. Mater. **748**, 177 (1998).

[19] Average Fe-Fe distances (Å) in Fe_6: 3.215 (*NN*), 5.563 (*NNN*), 6.425 (*NNNN*); in Fe_{10}: 3.028 (*NN*), 5.759 (*NNN*), 7.927 (*NNNN*), 9.318 (*NNNNN*), 9.798 (*NNNNNN*).

[20] D. Gatteschi and L. Pardi, Gazz. Chim. Ital. **123**, 231 (1993).

[21] A. Cornia, Ph.D. thesis, University of Modena, 1995.